Beam Physics Note
TRI-BN-20-13R
September 18, 2020

OLIS to RFQ Beam Transport and Acceleration in TRANSOPTR

Olivier Shelbaya

TRIUMF

Abstract: The TRIUMF Offline Ion Source provides the ISAC accelerator with stable pilot beams, used both for machine tuning and development, in addition to providing experiments with a diversity of stable species. The source has now been implemented in TRIUMF's HLA accelerator element database (`acc/`). Together with TRANSOPTR's novel radiofrequency quadrupole linac implementation, the present OLIS addition allows for the generation of continuous TRANSOPTR simulations of the ISAC-I post accelerator. In this report, the `acc/` database implementation of the OLIS, ILT and IRA beamlines, along with the positioning of the ISAC-RFQ in the database, is presented. Example envelope computations from OLIS through the RFQ and into the medium energy section (MEBT) of the ISAC-I accelerator are presented and future development steps identified.

4004 Wesbrook Mall, Vancouver, B.C. Canada V6T 2A3 Tel: 604 222-1047 www.triumf.ca

Contents

1 Introduction

This report documents the `acc/` database implementation of the transport beamlines connecting the ISAC offline ion source (OLIS) (Figure 1) to the ISAC linear accelerator's first main component, the radiofrequency quadrupole (RFQ). Having been verified from technical drawings, the database entry for the OLIS-RFQ can be used to easily generate `TRANSOPTR` files via the script `xml2optr`[1]. This work is part of a broader campaign to bring ISAC source and accelerator tuning under a state of agreement with model computations.

It is noteworthy that the report covering the OLIS implementation comes after work to add the remainder of the ISAC-I linac [1, 2, 3]. This has reflected challenges in the collection and interpretation of data and information about OLIS. Beamlines at the offline source require frequent maintenance, including physical cleaning of electrodes and other components. As such, it can be thought of as a relatively high traffic area, in terms of maintenance access.

There has been a corresponding need to modify the physical configuration of the beamline for matters of practicality during maintenance. As OLIS is a high subscription source, it is usually under constant operation, maintenance or development. But, the process of building and verifying the layout for a faithful model of the beam transport optics requires finding their dimensions and positions from design drawings.

As several discrepancies were found between drawings and the as-configured beamline [4], the recording of this work has correspondingly been delayed while verifications were carried out. Where necessary, corrective maintenance at OLIS has been requested to restore original device configuration [5]. The example of maintenance access encapsulates the reality of OLIS operation: it is driven by a need for fast, reproducible and reliable beam delivery. It is also true that operational tuning of the source is driven by such constraints and pressures. This report therefore aims to formalize the record of the OLIS to RFQ optics layout and present sources, in the form of TRIUMF Design Office technical drawings, which were used for this work.

With this addition to the `acc/` database, the ISAC accelerator is now fully in `TRANSOPTR`. This includes a novel RFQ simulation capacity [6] which therefore allows for continuous simulations from OLIS to the high energy beamlines of ISAC. This report will present a few such simulations, from OLIS through the RFQ and into the medium energy beamline (MEBT), demonstrating `TRANSOPTR`'s powerful potential when applied to the ISAC accelerator implementation. It is very important to note that the OLIS to RFQ tunes that will be presented herein are based entirely upon the work of R. Laxdal and R. Baartman, the designers of the OLIS and ILT-IRA beamlines, respectively. That the present `acc/`-database `TRANSOPTR` model of the beamlines reproduces the original design tunes when supplied with similar starting parameters and quadrupole settings is a further gauge of confidence.

[1] Credit: Paul Jung (TRIUMF/Waterloo) & Thomas Planche (TRIUMF)

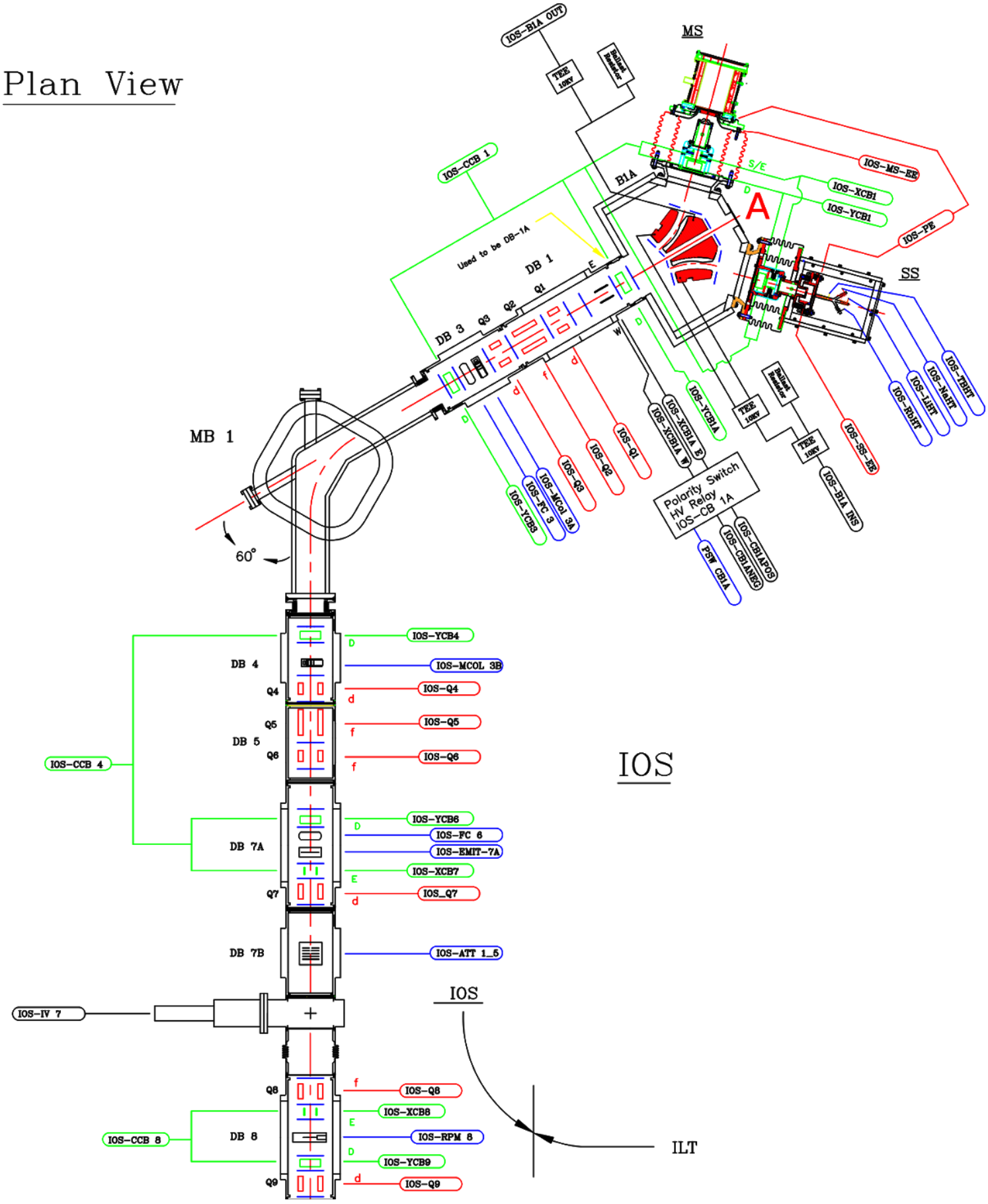

Figure 1: Sketch layout of the ISAC Offline Ion Source, showing transport optics, dipole magnet and 3-head attachment (top right). MCIS (not shown) connects to the 3-head bend at the location labeled A.

2 OLIS `acc/`-database Implementation

2.1 Ion Sources

Table 1 shows the sequence `ios_mcis`, representing the output of the multi charge ion source (MCIS/Supernanogan). The MCIS output is equipped with an Einzel lens (MCIS:EL1) of positive bias by design, which has been modelled in `Opera2D`.

sequence `ios_mcis`			
Start `IIS0378D.dwg` (x,y)		End `IIS0378D.dwg` (x,y)	
(29.17",19.23")		(12.02",19.23")	
Element Name	Element Type	s [mm]	length [mm]
start sequence	`marker`	0.0	0.0
MCIS:XCB1	`marker`	97.08	0.0
MCIS:YCB1	`marker`	138.36	0.0
MCIS:EL1	`AXEZ`	276.41	153.67
Start `ILE0378D.dwg` (x,y)		End `ILE0173D.dwg` (x,y)	
(262.83",98.35")		(309.75",98.35")	
IOS:B1A	`marker`	636.15	0.0
IOS:YCB1A	`marker`	872.12	0.0
IOS:XCB1A	`deflx`	960.00	50.80
end sequence	`marker`	1031.70	0.0

Table 1: Sequence `ios_mcis`, showing source design drawings (`.dwg` file) with reference start and end coordinates from which elements and their centerpoint positions along the optical axis. The `TRANSOPTR` element (subroutine) type, in addition to the element length are also displayed. All element positions are referenced to the drawing listed above their respective location in the table.

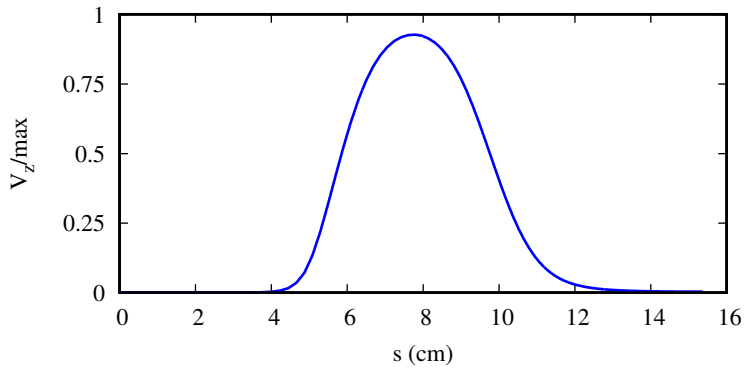

Figure 2: `Opera-2D` computed longitudinal electric potential for MCIS:EL1. The potential is used with `TRANSOPTR` subroutine `AXEZ`.

It is noted that there have been modifications made to the Einzel lens, and what is presented herein is only based on available design drawings. The longitudinal electric potential for EL1, normalized to the applied electrode voltage, is shown in Figure 2. The Einzel lens is implemented with optr subroutine `AXEZ`.

Next, Table 2 shows the sequence for the surface source and Table 3 microwave source.

sequence `ios_sis`			
Start `ISK4585D.dwg` (x,y)		End `ISK4585D.dwg` (x,y)	
(169.26",167.27")		(198.11",152.25")	
Element Name	Element Type	s [mm]	length [mm]
start sequence	`marker`	0.0	0.0
IOS:XCB1	`marker`	59.29	0.0
IOS:YCB1	`marker`	98.30	0.0
IOS:B1A	`eb`	457.86	159.46
IOS:YCB1A	`marker`	644.29	0.0
IOS:XCB1A	`deflx`	718.89	50.80
end sequence	`marker`	729.31	0.0

Table 2: Sequence `ios_sis`, showing source design drawings (`.dwg` file) with reference start and end coordinates from which elements and their centerpoint positions along the optical axis. The `TRANSOPTR` element (subroutine) type, in addition to the element length are also displayed. All element positions are referenced to the drawing listed above their respective location in the table.

sequence `ios_mws`			
Start `IIS0135D.dwg` (x,y)		End `IIS0135D.dwg` (x,y)	
(256.42",71.84")		(309.75",98.35")	
Element Name	Element Type	s [mm]	length [mm]
start sequence	`marker`	0.0	0.0
IOS:XCB1	`marker`	116.75	0.0
IOS:YCB1	`marker`	155.62	0.0
IOS:B1A	`eb`	400.96	159.46
IOS:YCB1A	`marker`	635.61	0.0
IOS:XCB1A	`deflx`	723.73	50.80
end sequence	`marker`	795.20	0.0

Table 3: Sequence `ios_mws`, showing source design drawings (`.dwg` file) with reference start and end coordinates from which elements and their centerpoint positions along the optical axis. The `TRANSOPTR` element (subroutine) type, in addition to the element length are also displayed. All element positions are referenced to the drawing listed above their respective location in the table.

2.2 OLIS Transport Line

Next, the OLIS to ILT transport line, featuring quadrupoles IOS:Q1 to IOS:Q6, and the 60° OLIS dipole magnet are featured in sequence `ios_db1.xml`, shown in Table 4. More information on the dipole can be found in reference [4]. Sequence `ios_db10` containing spherical benders IOS:B10/B13 is shown in Table 5, while the straight section to the ILE beamlines, sequence `ios_db14` is shown in Table 6.

sequence `ios_db1`			
Start `IIS0135D.dwg` (x,y)		End `IIS0135D.dwg` (x,y)	
(309.75",98.35")		(326.95",98.35")	
Element Name	Element Type	s [mm]	length [mm]
start sequence	`marker`	0.000	0.000
IOS:Q1	`equad`	91.48	52.35
IOS:Q2	`equad`	205.96	102.13
Start `IIS0192D.dwg` (x,y)		End `IIS0192D.dwg` (x,y)	
(42.90",30.33")		(84.41",176.30")	
IOS:Q3	`equad`	320.43	52.35
Start `ILE0173D.dwg` (x,y)		End `ILE0173D.dwg` (x,y)	
(-16.05",25.30")		(97.34",-0.85")	
IOS:MCOL3A	`slit`	390.49	0.00
IOS:MB	`mb`	1063.24	31.4041
IOS:MCOL3B	`slit`	1736.16	0.00
IOS:Q4	`equad`	1806.06	52.35
IOS:Q5	`equad`	1920.56	102.13
tomo-q6	`marker`	1985.20	0.0
IOS:Q6	`equad`	2035.07	52.35
IOS:Q7	`equad`	2497.04	61.62
IOS:Q8	`equad`	3177.69	61.62
IOS:RPM8	`marker`	3334.66	61.62
IOS:Q9	`equad`	3491.63	61.62
end sequence	`marker`	3535.73	0.000

Table 4: Sequence `ios_db1`, showing source design drawings (`.dwg` files) with reference start and end coordinates from which elements and their centerpoint positions along the optical axis. All element positions are referenced to the drawing listed above their respective location in the table.

Note that two calls to `fringeq` are added to `TRANSOPTR`. For quadrupoles IOS:Q1 to Q6:

```
call fringeQ(0.108,0.001,0.036,-0.260)
```

while for quadrupoles IOS:Q7, Q8 and beyond (ISAC electrostatic quadrupoles), the skimmer-electrode configuration produces fringe fields represented by:

```
call fringeQ(0.085,0.004,0.031,-0.232)
```

sequence ios_db10			
Start ISK4209d.dwg (x,y)		End ISK4209d.dwg (x,y)	
(280.69",-183.74")		(287.78",-214.17")	
Element Name	Element Type	s [mm]	length [mm]
start sequence	marker	0.000	0.000
IOS:B10	eb	184.38	199.49
tomo-q10	marker	421.758	0.0
IOS:Q10	equad	446.22	48.92
IOS:Q11	equad	516.07	36.22
IOS:RPM11	marker	597.09	0.0
IOS:Q12	equad	666.15	36.22
IOS:Q13	equad	736.01	48.92
IOS:B13	eb	997.89	199.49
end sequence	marker	1182.22	0.000

Table 5: Sequence ios_db10, showing source design drawings (.dwg files) with reference start and end coordinates from which elements and their centerpoint positions along the optical axis. All element positions are referenced to the drawing listed above their respective location in the table.

sequence ios_db14			
Start ILE1095D.dwg (x,y)		End ISK4209d.dwg (x,y)	
(434.67",-371.51")		(287.78",-214.17")	
Element Name	Element Type	s [mm]	length [mm]
start sequence	marker	0.000	0.000
IOS:B10	marker	189.82	0.0
IOS:Q14	equad	458.38	36.22
IOS:Q15	equad	528.23	48.92
IOS:Q16	equad	598.08	36.22
IOS:Q17	equad	947.46	36.22
IOS:Q18	equad	1017.31	48.92
IOS:Q19	equad	1087.16	36.22
end sequence	marker	1544.78	0.000

Table 6: Sequence ios_db14, showing source design drawings (.dwg files) with reference start and end coordinates from which elements and their centerpoint positions along the optical axis. All element positions are referenced to the drawing listed above their respective location in the table.

2.3 Select OLIS Beam Envelope Examples

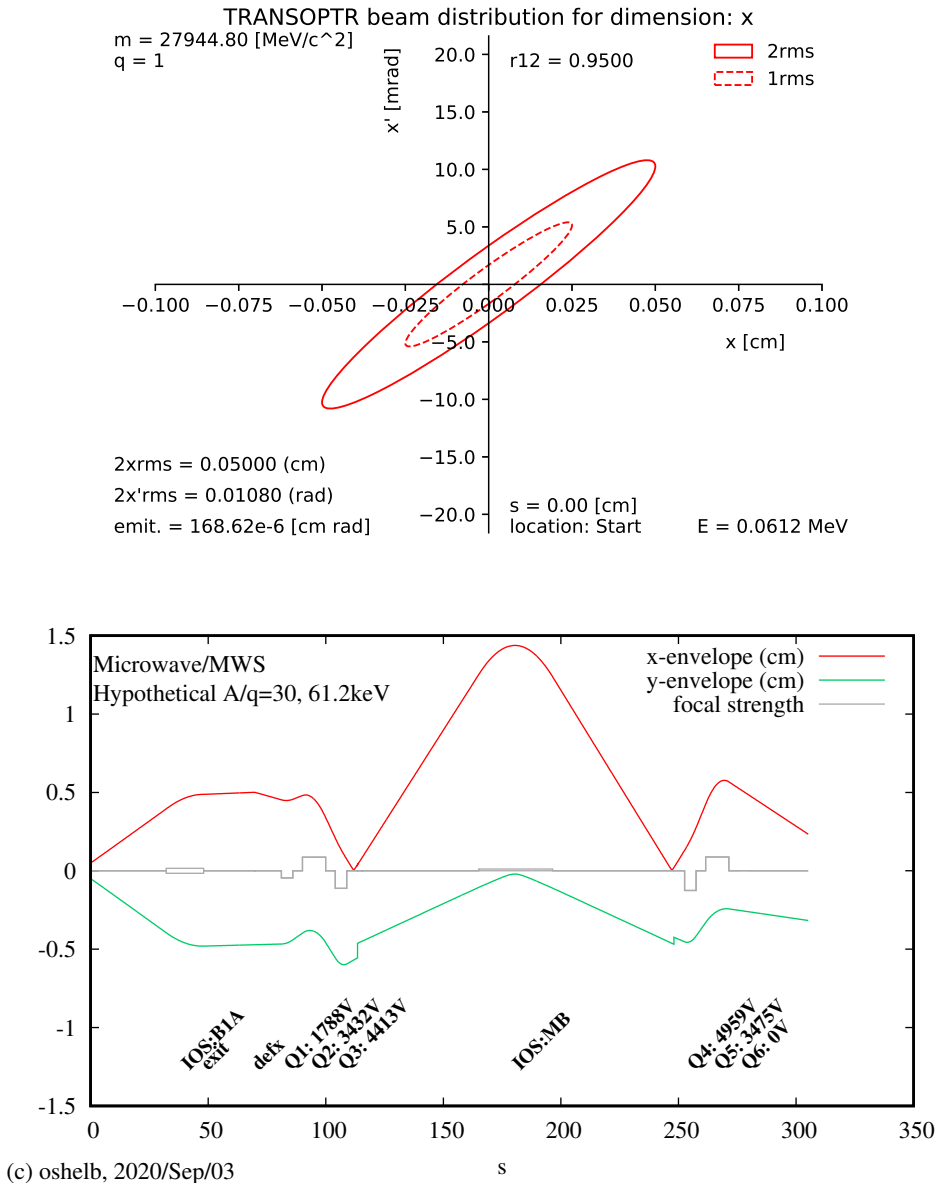

Figure 3: **Top:** MWS starting transverse beam distribution for horizontal (x) dimension. **Bottom:** MWS 2rms transverse envelopes for A/q = 30 beam at energy 61.2 keV, simulated up to IOS:FC6. Starting x and y beam parameters are identical.

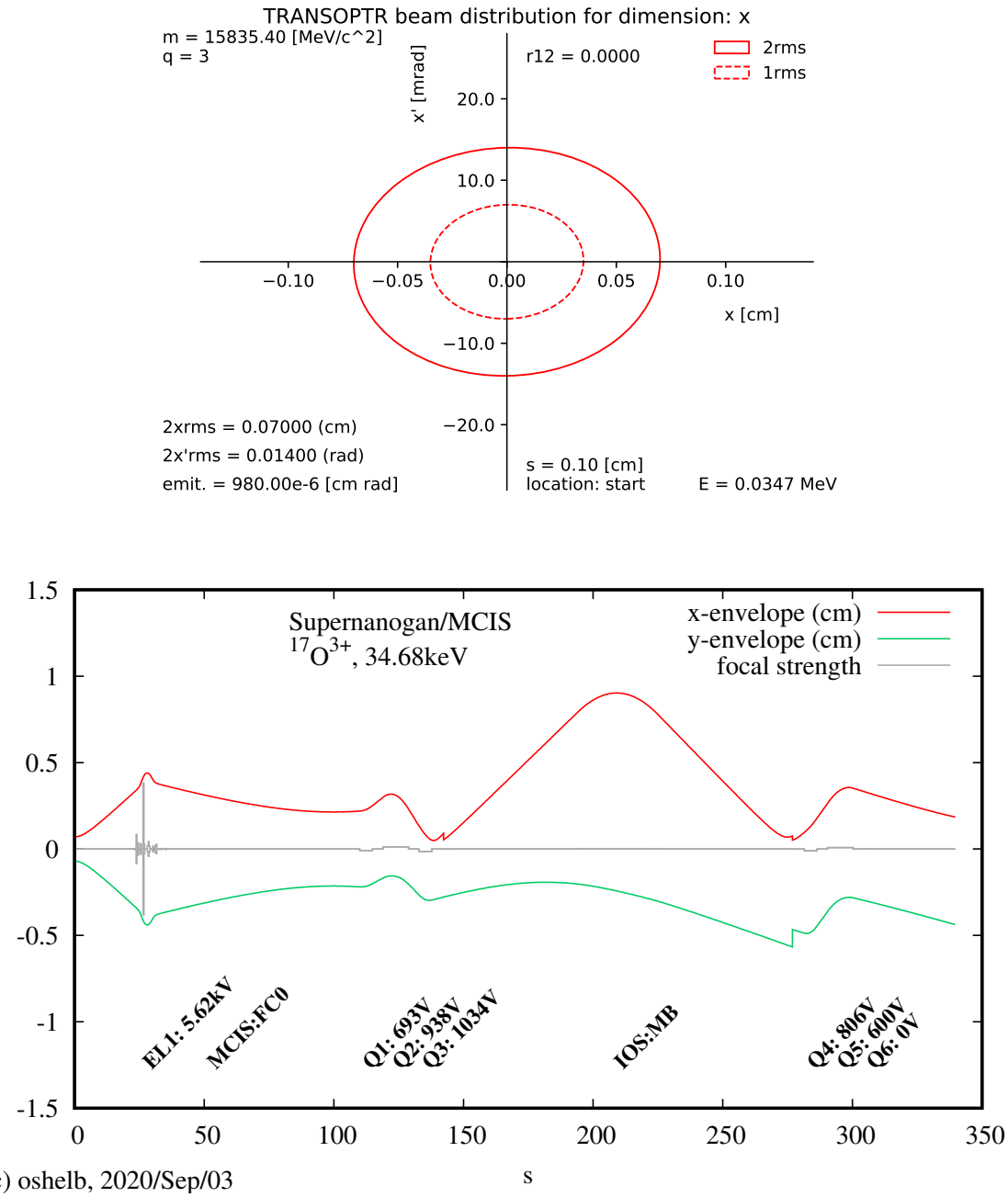

Figure 4: **Top:** MCIS starting transverse beam distribution for horizontal (x) dimension. **Bottom:** MCIS 2rms transverse envelopes for $^{17}O^{3+}$ beam at energy 34.68 keV, simulated up to IOS:FC6. Starting x and y beam parameters are identical.

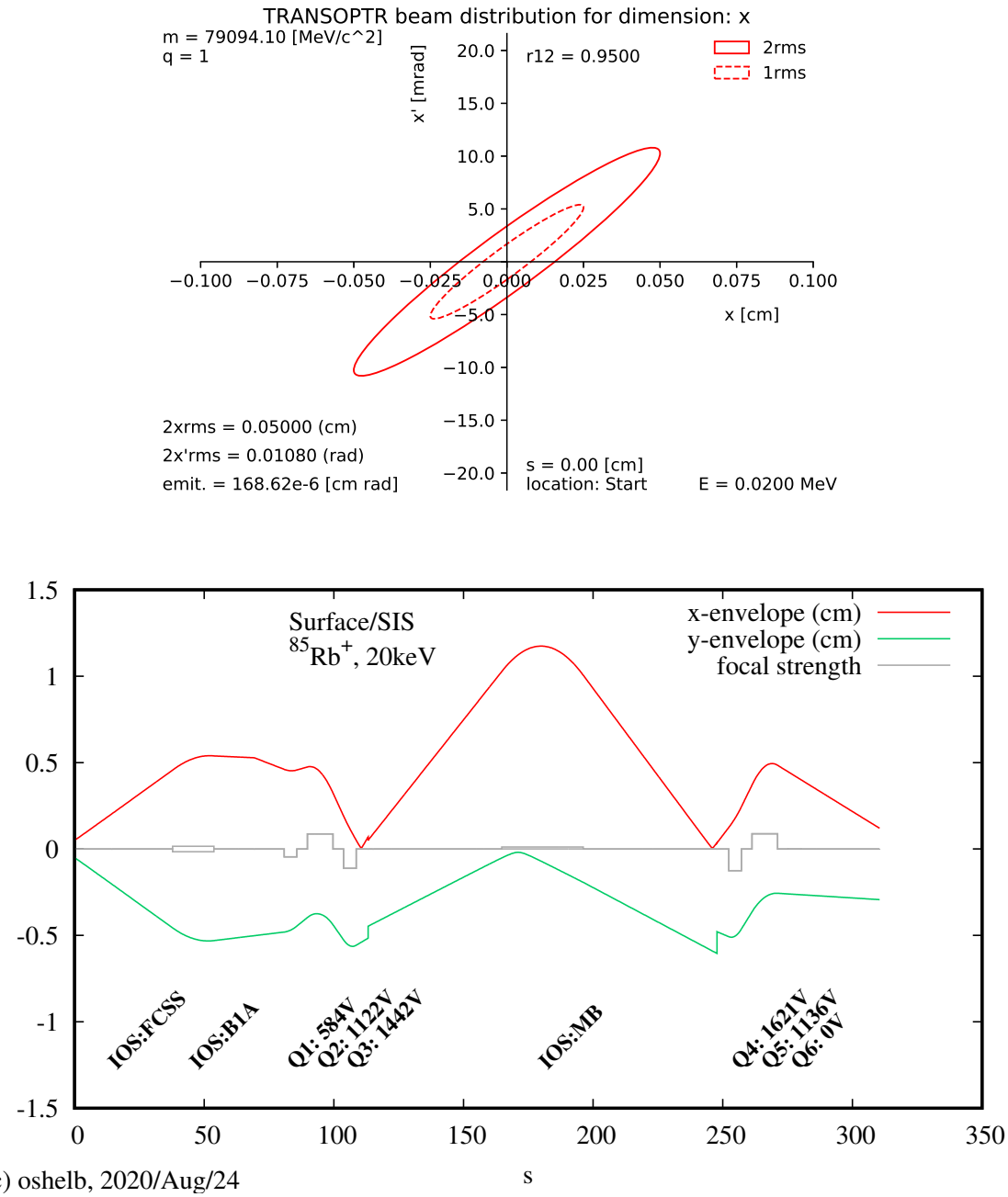

(c) oshelb, 2020/Aug/24

Figure 5: **Top:** SIS starting transverse beam distribution for horizontal (x) dimension. **Bottom:** SIS 2rms transverse envelopes for $^{17}O^{3+}$ beam at energy 34.68 keV, simulated up to IOS:FC6. Starting x and y beam parameters are identical.

3 ILT-IRA `acc/`-database Implementation

Transport to the ISAC linac through the ILT line follows the sequence `ios_db10.xml`, after the 45° bend at IOS:B13. The beamline segment starting at the spherical bender IOS:B10, including the ILT and IRA lines, terminating at the ISAC-RFQ is shown in Figure 7. Table 7 lists the recorded optical layout of the ILT and IRA lines, which terminate at the vacuum tank of the ISAC-RFQ. The sequence contains a marker representing the ISAC prebuncher (ISAC:PBN), which is implemented as a series of calls to `TRANSOPTR` subroutine `rfgap`. Diagnostic locations are listed in Table 8.

The ISAC RF Booster [7], a 3-gap device which allows for supplemental longitudinal phase space manipulation of beam prior to RFQ injection, is represented as a call to subroutine `linac`, with a field map shown in Figure 6. The device is located 1.3m upstream of the RFQ. The RF Booster's location is marked A in Figure 7. Development work on the booster implementation in `TRANSOPTR` remains underway as of writing and so its position is left approximate. A future implementation record will be published.

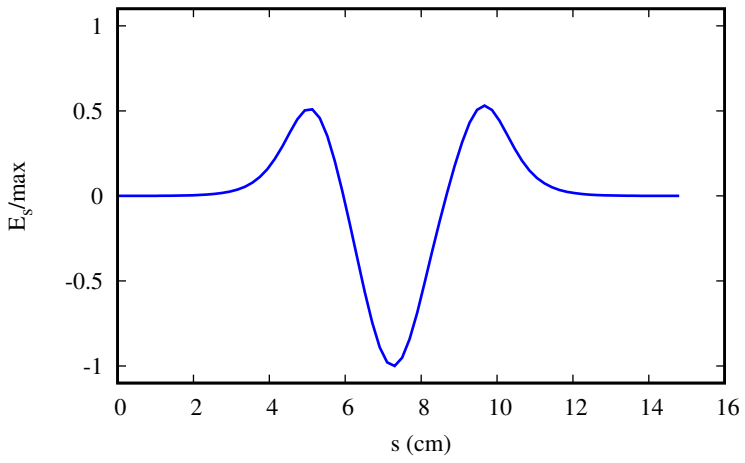

Figure 6: `COMSOL` simulated normalized on-axis electric field for the RF Booster. Provided by R. Laxdal.

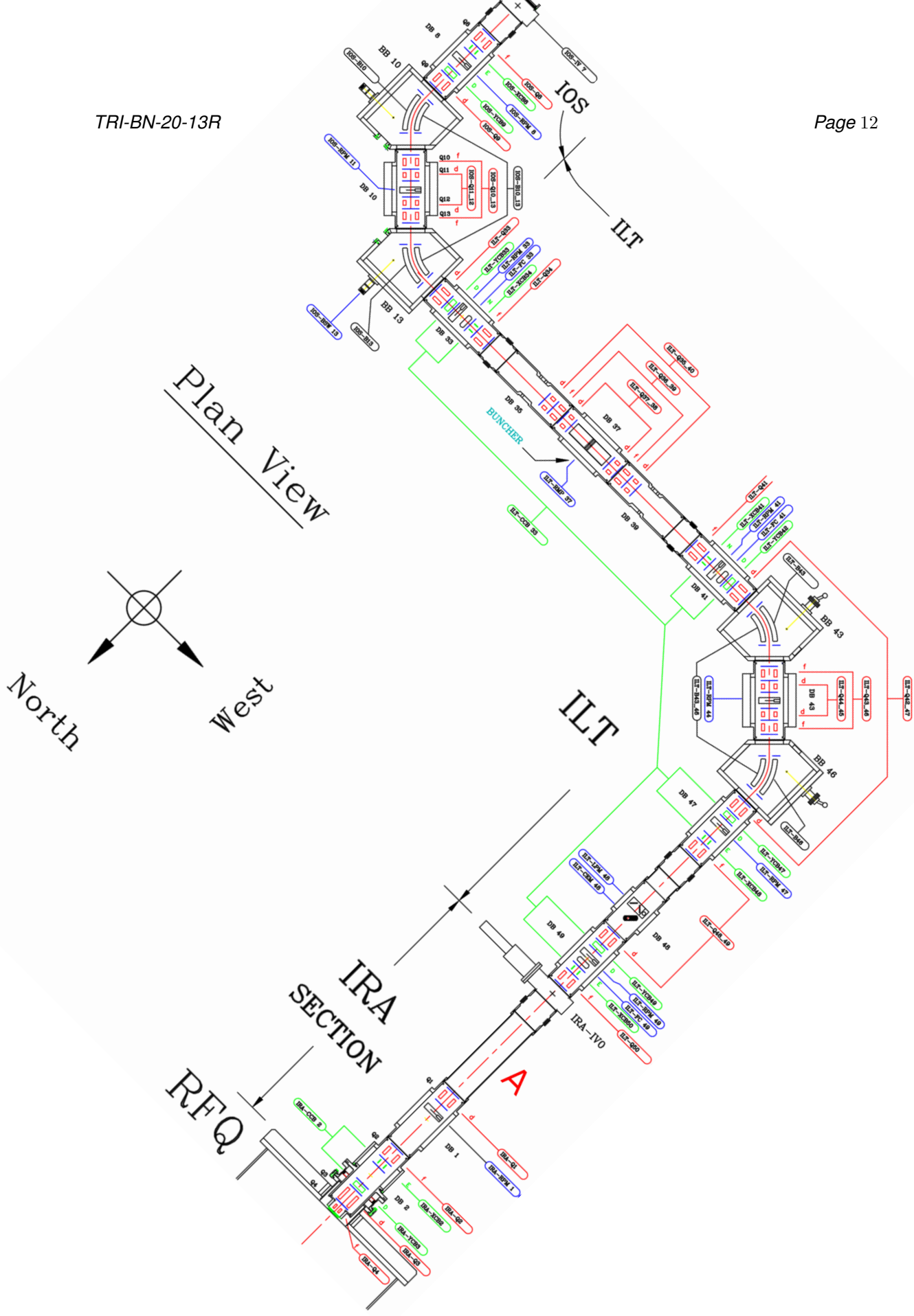

Figure 7: The OLIS(IOS)-ILT-IRA beamline, terminating at the ISAC-RFQ (bottom). Beam propagation occurs from top to bottom of the page. Approximate location of the RF Booster cavity (not shown in drawing) is at marker A.

sequence ilt_db33			
Start ISK4209d.dwg (x,y)		End ISK4209d.dwg (x,y)	
(291.11",-214.17")		(414.05",-366.51")	
Element Name	Element Type	s [mm]	length [mm]
start sequence	marker	0.000	0.000
tomo-q33	marker	12.65	0.0
ILT:Q33	equad	43.46	61.62
ILT:RPM33	marker	167.90	0.0
ILT:Q34	equad	357.43	61.62
ILT:Q35	equad	860.50	36.22
ILT:Q36	equad	930.35	48.92
ILT:Q37	equad	1000.20	36.22
ISAC:PBN	rf	1174.90	0.0
ILT:Q38	equad	1349.58	36.22
ILT:Q39	equad	1419.43	48.92
ILT:Q40	equad	1489.28	36.22
ILT:Q41	equad	1991.26	61.62
ILT:Q42	equad	2305.23	61.62
ILT:B43	eb	2534.16	199.49
ILT:Q43	equad	2796.00	48.92
ILT:Q44	equad	2865.85	36.22
ILT:Q45	equad	3015.96	36.22
ILT:Q46	equad	3085.81	48.92
ILT:B46	eb	3347.65	199.49
ILT:Q47	equad	3576.15	61.62
ILT:Q48	equad	3890.12	61.62
ILT:Q49	equad	4570.03	61.62
ILT:Q50	equad	4884.00	61.62
ISAC1:RFB	linac	5000.00	14.80
IRA:Q1	equad	5793.88	61.62
IRA:Q2	equad	6219.43	61.62
IRA:Q3	equad	6546.10	87.02
IRA:Q4	equad	6628.65	36.22
rotate -45°	rt	6546.10	87.02
ISAC1:RFQ	rfq	10530.56	760.13
end sequence	marker	14446.62	0.000

Table 7: Sequence ilt_db33, showing source design drawings (.dwg files) with reference start and end coordinates from which elements and their centerpoint positions along the optical axis. All element positions are referenced to the drawing listed above their respective location in the table.

(Diagnostics) sequence ilt_db33			
Start ISK4209d.dwg (x,y)		End ISK4209d.dwg (x,y)	
(291.11",-214.17")		(414.05",-366.51")	
Element Name	Element Type	s [mm]	length [mm]
start sequence	marker	0.000	0.000
ILT:RPM33	marker	167.90	0.0
ILT:RPM37	marker	1174.89	0.0
ILT:RPM41	marker	2132.31	0.0
ILT:RPM44	marker	2942.27	0.0
ILT:LPM48	marker	4401.41	0.0
ILT:CEM48	marker	4476.54	0.0
ILT:RPM49	marker	4711.03	0.0
IRA:RPM1	marker	5957.12	0.0
end sequence	marker	14446.62	0.000

Table 8: Sequence ilt_db33, showing source design drawings (.dwg files) with reference start and end coordinates from which elements and their centerpoint positions along the optical axis. All element positions are referenced to the drawing listed above their respective location in the table.

3.1 Positioning of The ISAC-RFQ

The addition to TRANSOPTR of an RFQ simulation capability is covered in more detail in [6]. An important consideration in the elaboration of sequence ilt_db33 is the centerpoint of the ISAC RFQ vane mapping, in addition to a frame rotation by 45°, owing to the relative tilt of the RFQ vanes. Previous RFQ simulation work by L. Root of the TRIUMF Beam Physics group in the form of Relax3D RFQ radial matching section simulations were used to determine the drift distance from quadrupole IRA:Q4 to the start of the radial matching section (RMS) of the RFQ vanes. From my notes, taken during analysis of L. Root's work, including original PARMTEQ simulations of the ISAC-RFQ:

```
RFQ 2term field map original length
is 760.13cm, which starts at the
beginning of the radial matching section.

From Larry Root's bnd_rms4.f Relax3D
simulation of the RFQ-RMS quotes a
drift distance of 6 refence cell lenghts
(first cell) from the outer tank-vacuum
wall up to the start of the vanes.
```

Using TRIUMF Design Office drawing ISK0141D.dwg, the distance from IRA:Q4 midpoint to the inner surface of the RFQ vacuum tank was determined. To this was added the known distance between the vacuum-tank wall to the starting of radial matching section. This position denotes the

starting point for the `TRANSOPTR` call to subroutine `rfqlinac`. The midpoint of the RFQ vanes in the `acc/` database is then half the total RFQ mapping file added to the s-coordinate of the RMS-start position. The s-position shown in Table 7 has been obtained in this manner.

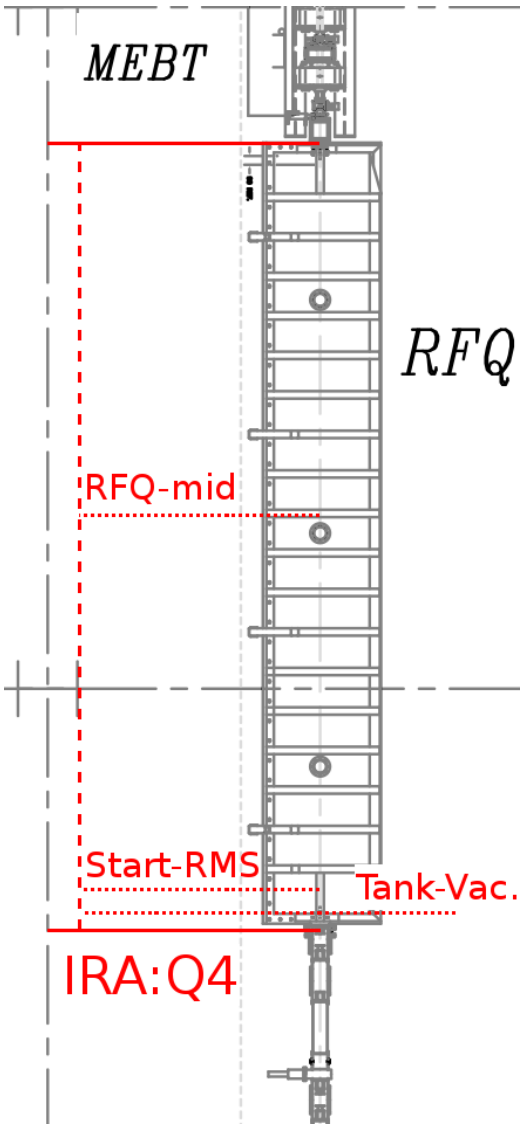

Figure 8: Positioning of the ISAC-RFQ vane mapping [6] with respect to quadrupole IRA:Q4. The end of sequence point line for `ilt_db33` is shown as a red line at the top of the ISAC-RFQ.

4 OLIS-MEBT Design Tune Demonstration

As a final demonstration of the present TRANSOPTR implementation, two tunes are presented from OLIS extraction up to MEBT:RPM5, downstream of the ISAC-RFQ. In both cases, the OLIS, ILT and IRA quadrupole settings were obtained from Rick Baartman and correspond to the design tunes provided by the beam physics group to RIB Operations. These are shown in Figure 10 for the microwave source and in Figure 11 for MCIS/Supernanogan. In both cases, starting beam distributions were identical as what was used for each source in Section 2.3.

The handling of the ISAC-prebuncher's conversion of a longitudinally continuous beam to a pre-bunched distribution at the entrance of the RFQ-RMS must be approximated. TRANSOPTR cannot account for nonlinearities introduced in the longitudinal phase space by the prebuncher harmonics. Instead, as an initial approximation, values from documented commissioning were used. Pre-bunched beams entering the RFQ have a recorded timespread of 5ns and an energy spread of 1% [8] when the prebuncher is optimally set. In TRANSOPTR, longitudinal units are in terms of (z, P_z)=$(\beta c\Delta t, \Delta E/\beta c)$. This works out to $(z, P_z) \sim$ (0.3cm,0.01).

A placeholder call to subroutine rfgap, providing an instantaneous and discrete kick, is made at the location of the ISAC-Prebuncher (Table 7). The RF gap frequency is fixed at 11.8 MHz, representing the first prebuncher harmonic. It is not expected that this faithfully replicate the reality of operating the ISAC prebuncher, though it does provide an approximate representation of longitudinal beam injection into the ISAC-RFQ.

An example of the ISAC prebuncher's longitudinal time-focus is shown in Figure 9. The three-harmonic prebunching introduces higher order effects to the longitudinal bunch distribution.

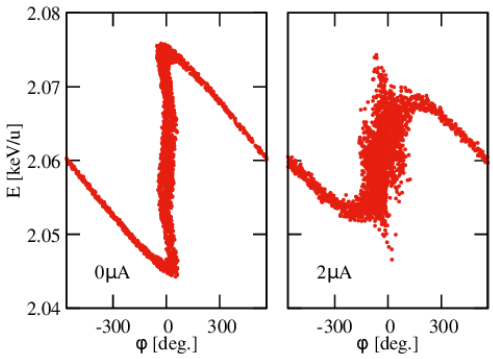

Figure 9: PARMELA simulation of ISAC-prebunching at entrance of ISAC-RFQ, showing time focus at both 0μA and 2μA beam currents.

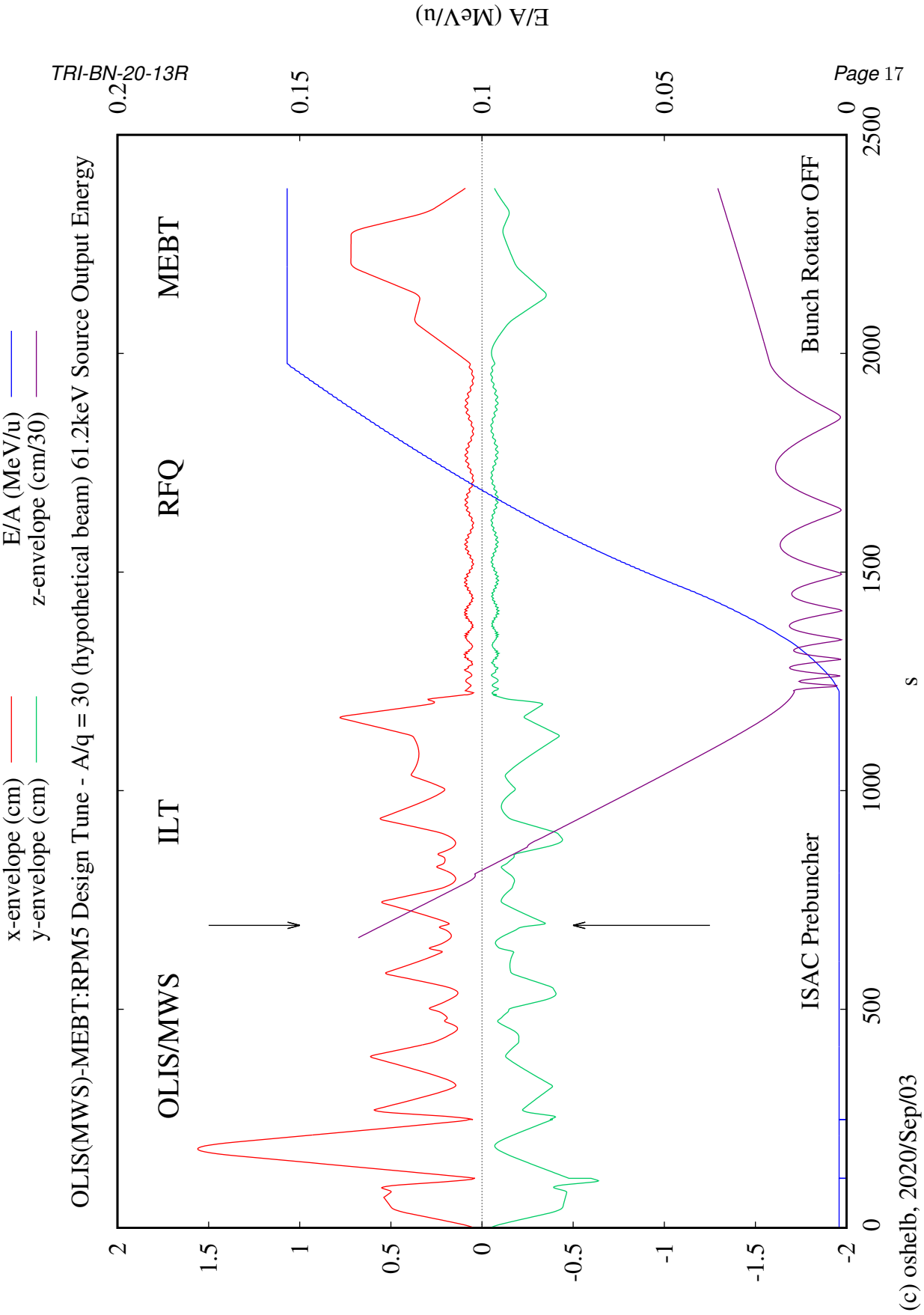

Figure 10: TRANSOPTR simulation of MWS extraction to MEBT:RPM5, following ISAC-RFQ acceleration. The transverse 2rms envelopes are shown, so is the reference particle energy. The present analysis excludes longitudinal envelopes. Starting x and y beam parameters are identical.

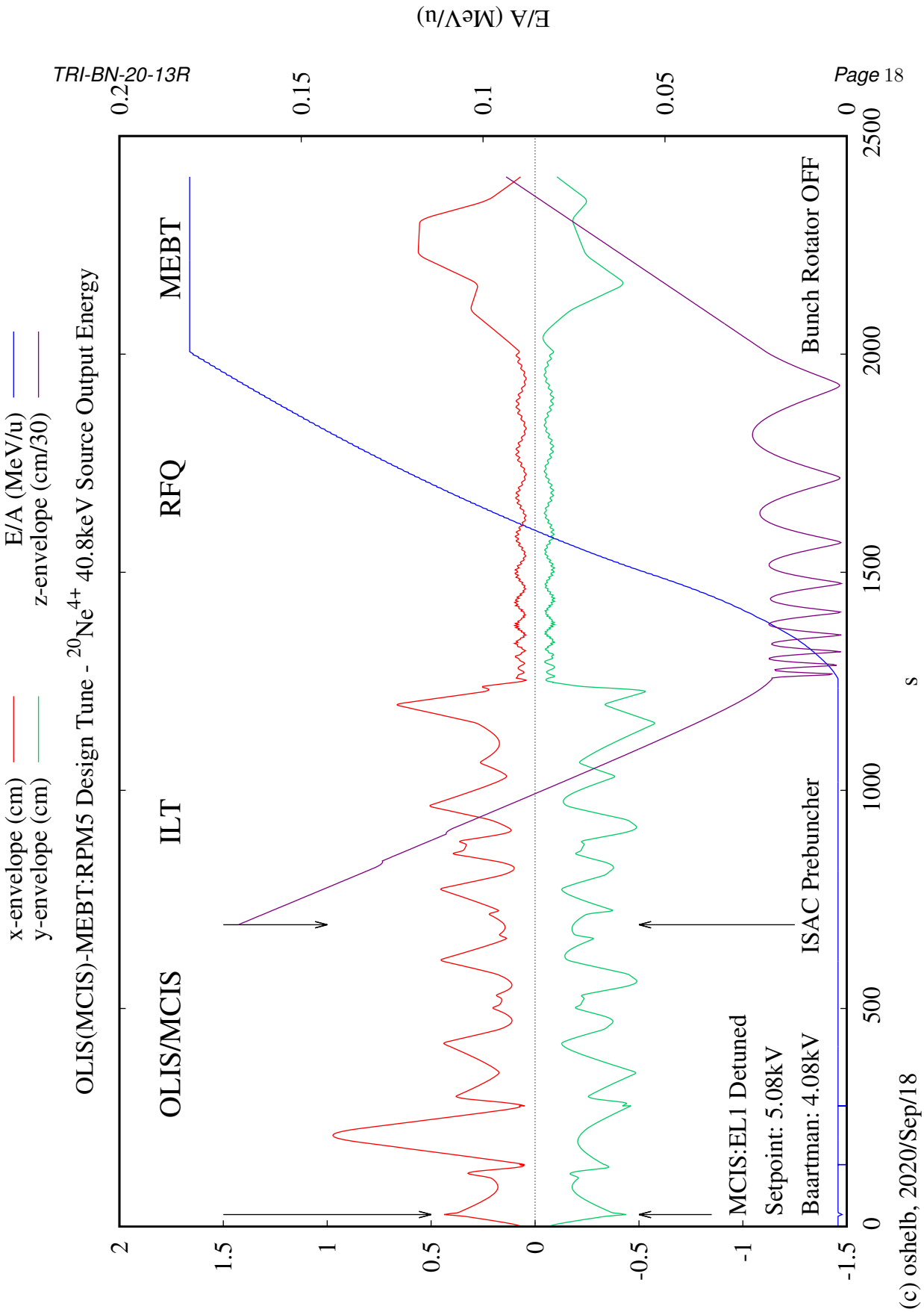

Figure 11: TRANSOPTR simulation of MCIS extraction to MEBT:RPM5, following ISAC-RFQ acceleration. The transverse 2rms envelopes are shown, so is the reference particle energy. The present analysis excludes longitudinal envelopes. Starting x and y beam parameters are identical.

5 Conclusion and Next Steps

The sequences detailed in this note complete the intial implementation of the ISAC-I accelerator in the TRIUMF-HLA `acc/` database. The envelope code is now capable of performing start-to-end simulations of the entire chain, in a single computation if needed. This is in no small part thanks to the recent addition to TRANSOPTR of an RFQ subroutine. Around this, the implementation of a faithfully built model, with dimensions drawn from design drawings produces a powerful tool for the ongoing development of model coupled accelerator tuning methods.

The tunes that have been shown in this report, most notably those of Figures 10 and 11 are the original design tunes for the low-energy section of the accelerator. Already, the simulations suggest an investigation of the Einzel lens at MCIS is in order. In Figure 11, it was necessary to detune the EL1 potential to 5.6kV, from a theoretical setpoint of 4.6kV. These model simulations suggest the MCIS-ILT tune should be investigated and possibly corrected. As it was found that changes were made to the offline ion source since the original tune computations [4, 5] were carried out by Baartman, the next steps in development will consist of performing on-line beam based tests for model comparison. This will eventually allow for the optimization of the on-line tune for the whole linac.

Work toward model-coupled accelerator tuning of the ISAC-I linac, using the start-to-end `TRANSOPTR` model of the machine and its beamlines will now be separated into transverse and longitudinal tune investigations. In the transverse case, measurements of the beam profile at diagnostics, in addition to quadrupole scan tomography will permit the evaluation of agreement between model and machine. In the OLIS case, this will also allow for a better understanding of output beams from the source. For the longitudinal case, calibration measurements are necessary to relate `TRANSOPTR`'s tuning parameters with those of the EPICS control system.

6 Acknowledgements

Thanks to Rick Baartman for the very significant assistance provided during this work, including on matters related to understanding `TRANSOPTR` (not to mention beam optics).. Rick, along with Oliver Kester patiently helped me navigate the addition of an RFQ simulation capacity to `TRANSOPTR`, an essential feature showcased in this work. Thomas Planche, Spencer Kiy, Paul Jung and Stephanie Rädel are thanked for their support, patience and advice throughout this project. This includes work toward the development of the TRIUMF HLA project as a whole, including the web interfaces and infrastructure around the `acc/` database in which the sequences documented herein are stored. Thanks to Tiffany Angus for patience, assistance and support during the course of the numerous OLIS investigations and tuning sessions that were necessary for this project to advance.

References

[1] Olivier Shelbaya. TRANSOPTR Implementation of the MEBT Beamline. Technical Report TRI-BN-19-02, TRIUMF, 2019.

[2] Olivier Shelbaya. TRANSOPTR Implementation of the HEBT Beamlines. Technical Report TRI-BN-19-06, TRIUMF, 2019.

[3] Olivier Shelbaya. The TRANSOPTR Model of the ISAC Drift Tube Linear Accelerator - Part I: Longitudinal Verification. Technical Report TRI-BN-20-08, TRIUMF, 2020.

[4] Olivier Shelbaya. Anomalous Operational OLIS Tunes. Technical Report TRI-BN-19-20, TRIUMF, 2019.

[5] Olivier Shelbaya. OLIS Maintenance Summary by Oli S. Technical Report TRI-BN-20-04, TRIUMF, 2020.

[6] O Shelbaya, R Baartman, and O Kester. Fast radio frequency quadrupole envelope computation for model based beam tuning. *Physical Review Accelerators and Beams*, 22(11):114602, 2019.

[7] Robert Laxdal, Zhengting Ang, Thomas Au, Spencer Kiy, Stephanie Rädel, Olivier Shelbaya, Vladimir Zvyagintsev, et al. A 3-gap booster cavity to match ion source potential to rfq acceptance. In *29th Linear Accelerator Conf.(LINAC'18), Beijing, China, 16-21 September 2018*, pages 196–199. JACOW Publishing, Geneva, Switzerland, 2019.

[8] R Laxdal, R Baartman, P Bricault, G Dutto, K Fong, K Jayamanna, M MacDonald, G Mackenzie, R Poirier, W Rawnsley, et al. First beam test with the isac rfq. In *This conference*, 1998.